

Spring 5-31-2003

## Graphical user interface for improved laser eye surgery

Venkata K. Kuruganti  
*New Jersey Institute of Technology*

Follow this and additional works at: <https://digitalcommons.njit.edu/theses>



Part of the [Computer Engineering Commons](#)

---

### Recommended Citation

Kuruganti, Venkata K., "Graphical user interface for improved laser eye surgery" (2003). *Theses*. 626.  
<https://digitalcommons.njit.edu/theses/626>

This Thesis is brought to you for free and open access by the Electronic Theses and Dissertations at Digital Commons @ NJIT. It has been accepted for inclusion in Theses by an authorized administrator of Digital Commons @ NJIT. For more information, please contact [digitalcommons@njit.edu](mailto:digitalcommons@njit.edu).

## Copyright Warning & Restrictions

The copyright law of the United States (Title 17, United States Code) governs the making of photocopies or other reproductions of copyrighted material.

Under certain conditions specified in the law, libraries and archives are authorized to furnish a photocopy or other reproduction. One of these specified conditions is that the photocopy or reproduction is not to be “used for any purpose other than private study, scholarship, or research.” If a user makes a request for, or later uses, a photocopy or reproduction for purposes in excess of “fair use” that user may be liable for copyright infringement,

This institution reserves the right to refuse to accept a copying order if, in its judgment, fulfillment of the order would involve violation of copyright law.

**Please Note: The author retains the copyright while the New Jersey Institute of Technology reserves the right to distribute this thesis or dissertation**

Printing note: If you do not wish to print this page, then select “Pages from: first page # to: last page #” on the print dialog screen

The Van Houten library has removed some of the personal information and all signatures from the approval page and biographical sketches of theses and dissertations in order to protect the identity of NJIT graduates and faculty.

## **ABSTRACT**

### **GRAPHICAL USER INTERFACE FOR IMPROVED LASER EYE SURGERY**

by  
**Venkata K. Kuruganti**

This thesis develops a system for laser eye surgery that is a significant improvement over existing technology. The new system uses image matching and MEMS micromirrors to introduce feedback control, automation and record keeping to the laser surgery process, eliminating the unwanted effects of eye movement during surgery and introducing a wide range of other benefits. It is expected that this improvement can be implemented as an addition to existing systems as well as a foundation for new tools, perhaps even remote, internet enabled ones.

The basic components of the new system are described and demonstrated, including image matching between reference and real-time images through well-known algorithms, application of matching information to generate control voltages to lock positioning and firing LASER onto selected locations on the eye using electrostatically controlled micromirrors, and characterization of the micromirrors for this application. This thesis focuses particularly on the development of a prototype graphical user interface that integrates image capture, image matching, mirror control, and user interaction into a single unit.

**GRAPHICAL USER INTERFACE  
FOR IMPROVED LASER EYE SURGERY**

by  
**Venkata K. Kuruganti**

**A Thesis  
Submitted to the Faculty of  
New Jersey Institute of Technology  
In Partial Fulfillment of the Requirements for the Degree of  
Master of Science in Computer Engineering**

**Department of Electrical and Computer Engineering**

**May 2003**

Blank Page

**APPROVAL PAGE**  
**GRAPHICAL USER INTERFACE**  
**FOR IMPROVED LASER EYE SURGERY**

**Venkata K. Kuruganti**

5/22/03

---

Dr. Kenneth R. Farmer, Thesis Advisor Date  
Associate Professor of Physics, NJIT

5/22/03

---

Dr. Edwin Hou, Committee Member Date  
Associate Professor of Electrical and Computer Engineering, NJIT

5/22/03

---

Dr. Sven Loncaric, Committee Member Date  
Assistant Professor of Electrical and Computer Engineering, NJIT

5/22/03

---

Dr. Neelakshi Bhagat, Committee Member Date  
Assistant Professor of Ophthalmology, New Jersey Medical School

## BIOGRAPHICAL SKETCH

**Author:** Venkata K. Kuruganti

**Degree:** Master of Science

**Date:** May 2003

**Date of Birth:**

**Place of Birth:**

### **Undergraduate and Graduate Education:**

- Master of Science in Computer Engineering  
New Jersey Institute of Technology, Newark, NJ 07102, 2003
- Bachelor of Engineering in Electronics and Communication Engineering  
Dr. M.G.R. Engineering College, Chennai, India, 2000

**Major:** Computer Engineering



To my beloved family and friends

## **ACKNOWLEDGEMENT**

I would like to take this opportunity to express my wholehearted appreciation for my research advisor, Dr. Kenneth R. Farmer, for providing me with the opportunity to be involved in this research. His encouragement and support have played a key role in all accomplishments.

I would like to thank my colleague, Mr. Narashiman Chakravarthy, for his support all through the research work.

I would like to thank Dr. Neelakshi Bhagat for her support and encouragement, all through the research work. I appreciate it very much. I am looking forward to working with her in future.

I would like to thank Dr. Edwin Hou and Dr. Sven Loncaric for serving on my thesis committee.

## TABLE OF CONTENTS

Chapter	Page
1 INTRODUCTION.....	1
1.1 Introduction.....	1
1.1.1 Macular Degeneration.....	1
1.1.2 Current Surgical Procedure.....	1
1.2 Motivation.....	3
1.2.1 Nystagmus.....	3
1.2.2 Micro-Electro-Mechanical-Systems.....	4
1.3 Why is Tracking Important?.....	5
1.3.1 What are the Potential Improvements?.....	5
1.4 Scope of the Thesis.....	6
2 PROPOSED SYSTEM.....	7
2.1 Proposed System.....	8
2.1.1 Video Camera.....	8
2.1.2 Computer.....	9
2.1.3 Signal Conditioner.....	10
2.1.4 MEMS Mirrors.....	10
3 THE ELECTROSTATIC MICROACTUATOR.....	11
3.1 Introduction.....	11
3.2 Characterization.....	12

**TABLE OF CONTENTS**  
**(Continued)**

<b>Chapter</b>	<b>Page</b>
3.3 Microactuator Dimensions.....	12
3.3.1 Dimensions of the Actuator Plate.....	16
3.3.2 Dimensions of the Actuator Spring.....	18
3.3.3 Resonant Frequency of the Microactuator.....	20
3.4 Dynamic Characteristics of the Microactuator.....	20
3.4.1 Snapdown Voltage.....	20
3.4.2 Experiment to Determine the Snapdown Voltage of the Microactuator..	21
4 EYE TRACKING ALGORITHM AND GRAPHICAL USER INTERFACE.....	25
4.1 Tracking Algorithms.....	25
4.1.1 Exclusion Area Algorithm.....	25
4.1.2 Eye Tracking Algorithm.....	25
4.1.3 Hybrid Algorithm.....	26
4.2 Aspects to Consider for Eye Tracking.....	27
4.2.1 Translation.....	27
4.2.2 Rotation.....	28
4.2.3 Scaling.....	29
4.3 Tracking the Eye.....	32
4.3.1 Registration.....	33
4.3.2 Implementing the Registration.....	34
4.4 The Graphical User Interface.....	36

**TABLE OF CONTENTS**  
**(Continued)**

<b>Chapter</b>	<b>Page</b>
5 CONCLUSION.....	38
6 FUTURE SCOPE.....	39
6.1 Aspects of Retinal Movement.....	39
6.2 Incorporating the CALS in the Existing Surgical Equipment.....	39
6.3 Additional Features in the Graphical User Interface.....	40
6.3.1 History of Surgical Procedure.....	40
6.3.2 Computer Controlled LASER.....	40
6.3.3 More User-Friendly Graphical User Interface.....	40
6.4 Remote Operation.....	41
APPENDIX A MACULAR DEGENERATION.....	42
APPENDIX B FABRICATION OF THE MEMS MIRROR.....	44
APPENDIX C REGISTRATION ALGORITHMS.....	50
REFERENCES.....	51

## LIST OF TABLES

<b>Table</b>		<b>Page</b>
3.1	Dimensions of the Microactuator.....	16

## LIST OF FIGURES

Figure	Page
2.1 Schematic of the proposed setup.....	8
3.1 The electrostatic microactuator (micro mirror).....	11
3.2 Profilometer image.....	13
3.3 Top view of the microactuator.....	14
3.4 X profile of microactuator.....	15
3.5 Y profile of microactuator.....	15
3.6 Portions of the microactuator.....	16
3.7 Top view when the microactuator is in snapdown position.....	17
3.8 Y profile of microactuator in snapdown position.....	17
3.9 Top view of actuator spring.....	18
3.10 X profile of actuator spring.....	19
3.11 Y profile of actuator spring.....	19
3.12 Voltage is applied between the actuator plate and substrate.....	21
3.13 Experimental setup to determine snapdown voltage of actuator.....	22
3.14 Actuator plate and adjoining polished surface.....	23
3.15 Geometric analogy for the experimental setup.....	23
4.1 The translation movement of an object. RoI is the Region of Interest.....	27
4.2 The rotation of the object along the axis of image capture. The shaded region is the RoI.....	28
4.3 Scaling of the image.....	29

**LIST OF FIGURES  
(Continued)**

<b>Figure</b>	<b>Page</b>
4.4 Target area (Sub-Retinal-Neo-Vascularization) on the retina (a) fluorescein angiogram (b) microscopic image.....	30
4.5 Reference areas on (a) fluorescein angiogram (b) microscopic image.....	31
4.6 Reference areas on (a) fluorescein angiogram (b) real-time image (RTI).....	32
4.7 Images should look identical for the sum of the squared differences algorithm to work with accuracy.....	33
4.8 Grayscale version of the real-time image.....	34
4.9 Inverted grayscale version of the real-time image.....	35
4.10 The Graphical User Interface.....	36
B.1 Etched pit on the Silicon wafer. This forms the cavity under the actuator plate.	44
B.2 Growth of SiO <sub>2</sub> on the wafer.....	45
B.3 SiO <sub>2</sub> is grown on a thin Silicon wafer. This makes the wafer bonding easier...	46
B.4 The thin Silicon wafer is fusion bonded on the first wafer.....	47
B.5 Actuator plate patterned on the bonded thin Silicon.....	48
B.6 Gold and Chromium deposition on the actuator structure, to provide a polished surface and good electrical contact.....	49



# CHAPTER 1

## INTRODUCTION

### 1.1 Introduction

#### 1.1.1 Macular Degeneration

Macular degeneration [1] refers to the condition wherein damage occurs in the blood vessels in the retina due to aging. More information about macular degeneration is available in the appendix.

Currently, macular degeneration is treated by a surgical procedure that uses a **LASER (Light Amplification by Stimulated Emission of Radiation)** to treat the damaged portions of the retina.

#### 1.1.2 Current Surgical Procedure

The current retinal eye surgery using a LASER<sup>[2]</sup> is a two-step process. The first step is to identify the problem area in the eye, *i.e.*, to identify what are known as Sub-Retinal-Neovascularization (new blood vessels growing under the retina which will leak and bleed) or SRNV. This is done by performing fluorescein angiography. The second step is to destroy the SRNV using a LASER.

**1.1.2.1 Fluorescein Angiography.** Fluorescein angiography is a procedure that allows the blood vessels in the back of the eye to be photographed by injecting a fluorescent dye into the bloodstream. The fluorescent dye is injected through the hand or arm.

Fluorescein angiography is performed to:

1. Perform diagnosis.
2. Obtain a permanent record of the anatomy of the eye.
3. Have a reference when performing the eye surgery.

Fluorescein sodium is a commonly used dye. It is a highly fluorescent, synthetic, sodium salt of Fluorescein, which absorbs blue light with fluorescence.

The pupils will be dilated with eye drops and the dye is injected into a vein in the patient's arm. Following the injection, photos are taken quickly over a period of about sixty seconds as the dye enters the vessels at the back of the eye.

Interpretation of the abnormal angiogram relies on the identification of areas that exhibit hypo fluorescence (darkness) or hyper fluorescence (brightness). These are descriptive terms that refer to the time specific, relative brightness of fluorescence in comparison with a normal study. There is usually a gap of two to three weeks from when the FA is performed, to the time when the LASER eye surgery is performed.

**1.1.2.2 The Retinal Eye Surgery.** About two weeks after the fluorescein angiography, the retinal eye surgery is performed using LASER. The specifications of the LASER used for the procedure depend on the patient's condition and disease. The LASER's regularly used are Argon LASER for Green, which is not very powerful; and Krypton LASER for Red, more powerful than the Argon LASER.

When the retinal eye surgery is performed using a LASER, a portion of the target area (SRNV) is first aimed at, using a slit lamp [3] microscope. To identify the SRNV, the fluorescein angiogram image is used as a reference. The SRNV are identified by their relative distance from the identifiable features on the image of the eye, visible through

the slit lamp microscope. Once the target area is properly aimed at, the LASER is fired at the target area. This is performed repeatedly to fire LASER across the whole of the SRNV.

The current LASER treatment is recommended only in rare cases of macular degeneration. This form of treatment is feasible only when the abnormal blood vessels are far away enough from the sensitive portions of the eye such as the fovea, or optic nerve that they are not damaged. If these portions are damaged, the patient loses vision. Only rare cases of macular degeneration meet these criteria. When LASER treatment is possible, it may slow or stop the progression of the disease.

## **1.2 Motivation**

### **1.2.1 Nystagmus**

When the LASER eye procedure is performed, the patient's eye is sedated. This does not mean that the eye remains totally stationary. There is an involuntary motion of the eye, even under sedation. This motion is known as *Nystagmus*.

Nystagmus results in the eye moving in a random manner. When the LASER eye procedure is performed, a reference beam of light is placed on the desired area where the LASER has to be fired. After the desired area has been aimed at, the LASER is fired. If the eye moves randomly when the LASER is fired, the LASER will not strike the desired area. As a result, the LASER might strike the fovea, resulting in the patient losing vision.

The proposed solution is to use a computer controlled mirror to guide the LASER onto the desired area on the retina. The computer would track the movement of the eye using an image matching technique that compares the reference fluorescein angiogram to a real-time image of the eye, while the guidance system would precisely guide the LASER onto the desired area.

### **1.2.2 Micro-Electro-Mechanical-Systems**

Micro-Electro-Mechanical-Systems (MEMS) are devices fabricated employing the lithography techniques used in the fabrication of integrated circuits<sup>[4]</sup>. The advanced fabrication techniques developed for circuit fabrication enable easy fabrication of MEMS devices. MEMS devices can be used to guide the LASER because of the following reasons:

1. Can be fabricated easily.
2. Reliability.
3. Accuracy.
4. Can be computer controlled easily.

### **1.3 Why is Tracking Important?**

During the retinal eye surgery, the eye movement is minimized by sedation, before performing the surgery. However, there are minute, involuntary movements of the eye. These movements are called saccadic movements of the eye. Due to these movements, the LASER may not fall precisely on the target area even after aiming using the slit lamp microscope.

The distance from the macula or optic nerve, to the SRNV is of the order of microns. This means that the saccadic movements the eyes are comparable to the dimensions of the LASER. To overcome this problem, currently, the duration of individual LASER pulses is kept low. This means that the number of required LASER pulses is high. Moreover, this is not a perfectly fail proof mechanism since the laser can accidentally be fired onto critical features such as the fovea or optic nerve.

#### **1.3.1 What are the Potential Improvements?**

To overcome these problems, several approaches can be followed:

1. Track the movements of the eye and enable/disable the LASER if the target area goes outside the locked area.
2. Track the movements of the eye and add correction factors for the X and Y coordinates of the LASER, in effect stabilizing the image for the operator. This would be a semiautomatic process where the operator (surgeon) will be selecting the individual portions on the SRNV before the LASER is fired.
3. Allow the operator to select the whole of the area where the LASER is to be fired; and then perform automatic locking, tracking and firing of the LASER on the individual portions. This approach does not have human intervention.

## 1.4 Scope of the Thesis

In this thesis work, the feasibility and nuances of the approaches are explored.

The thesis work involves the following:

1. Propose a system for computer assisted LASER surgery.
2. Characterize various MEMS electrostatic microactuators and determine compatibility of the device for the application.
3. Develop an algorithm that compensates for the eye movements. This is a feature aspect of this thesis. The aim is to produce a graphical user interface (GUI) that clearly demonstrates the improvements enabled by the combined MEMS/image matching process.

## **CHAPTER 2**

### **PROPOSED SYSTEM**

The Computer Assisted LASER Surgical (CALs) system is a feedback control system.

As in any feedback control system, there are the three variables:

1. Set point.
2. Control Variable.
3. Process variable.

In this system, the process variable is the position of the target area on the retina; the set point is the place the operator wants to point the LASER; and the control variable is the position of the aiming beam on the retina. The process variable is not affected by the control action. However, the movement of the retina is compensated by moving the aiming beam. In effect, the movement of the target area is nullified. The CALs system has to perform the following tasks:

1. Capture the image of the eye.
2. Determine the displacement of the eye from its initial position.
3. Compensate for the movement of the eye by reaiming MEMS micromirrors.

## 2.1 Proposed System

The system schematic shown in Figure 2.1 can accomplish the required tasks.

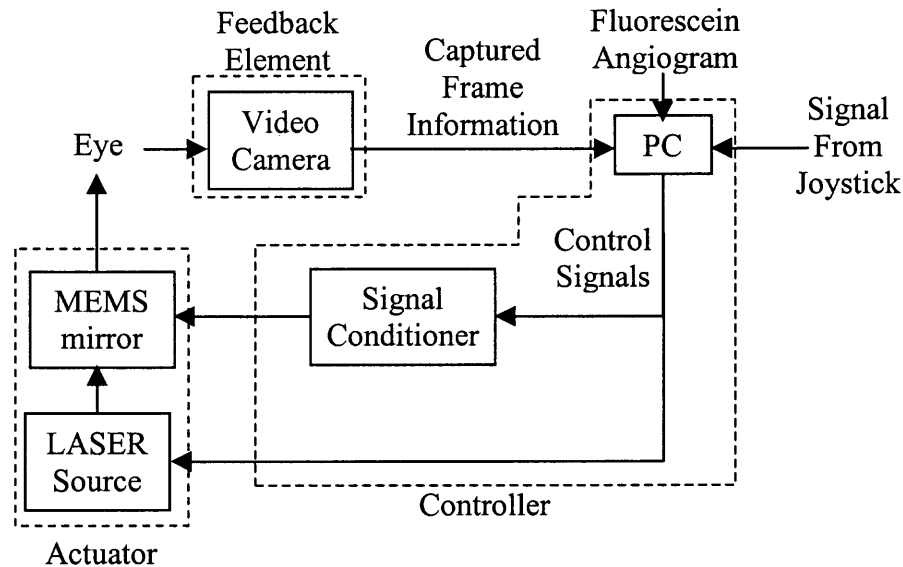


**Figure 2.1** Schematic of the proposed setup.

As in any feedback control system, this setup has three components. The components and their roles in the system can be listed as follows:

1. Feedback element: Video camera (with comparison to reference fluorescein angiogram or FA image).
2. Controller: Computer and signal conditioner.
3. Actuator: LASER source and MEMS mirrors.

### 2.1.1 Video Camera

The video camera captures the image of the retina. To accomplish the task properly, the camera has to satisfy the following requirements.

1. Interface circuitry: An interface circuitry is required to allow communication between the computer and the camera.



2. Digital output: The computer understands only digital (binary) information. The output of the camera should be digital information.
3. Programmable: The camera should be programmable. This means that the camera should be able to transmit a frame of information whenever the computer requests it.
4. Compatibility: The package used for the control algorithm should also support the camera.
5. Cropping: The video information obtained from the camera should have dimensions that are compatible with the fluorescein angiogram (FA) image. If this is not the case, cropping or scaling of the image should be possible.

### **2.1.2 Computer**

The computer captures the video information, frame by frame and performs the control action. This can be broken into the following steps.

1. Gather video frame from the video camera. This frame is referred to as the *real time image* or *RTI*.
2. Crop the image into the required size.
3. Compare the RTI with the FA image.
4. Determine the displacement of the eye.
5. Compensate for the movement by generating the corresponding difference voltages for the MEMS mirrors.

Apart from these tasks, the RTI is also displayed on the monitor. This allows the operator to observe the laser procedure better, and visualize the actions taken. In theory,

the operator can perform the procedure on the monitor and the computer can reflect the operator's actions on the surgical system.

### **2.1.3 Signal Conditioner**

Depending on the mirror design, as discussed in a later chapter (Chapter 3), the operating voltage of the mirror is between 10V and 40V. This is too high to be generated using the computer. This is overcome by using the signal conditioner. The signal conditioner amplifies the output of the computer, to bring it to the operating range of the mirrors.

### **2.1.4 MEMS Mirrors**

The MEMS mirrors deflect the LASER onto the retina. In reference to the system, the mirrors are not the intelligence, but just the actuators. However, their physical characteristics (Chapter 3) are the key to accomplish the compensation for the eye movements. If no mirrors are used, the LASER source will have to be moved to compensate. This is impractical, and too slow to be effective. The small size of the mirrors gives the edge required to accomplish the task.

Before a MEMS mirror can be used for the application, it has to be characterized to verify its compatibility for the application. Chapter 3 focuses on characterization of the MEMS electrostatic microactuator.

## CHAPTER 3

### THE ELECTROSTATIC MICROACTUATOR

#### 3.1 Introduction

The electrostatic microactuator is a MEMS device that has moving parts. It has a flat reflective surface (mirror plate) held in place by two torsion springs. A cavity is present under the plate. Whenever a potential difference is applied between the plate and the substrate, the plate deflects into the cavity, due to electrostatic force of attraction. These microactuators are addressed as variable angle mirrors or micro mirrors. Figure 3.1 illustrates the various parts of the micro mirror.

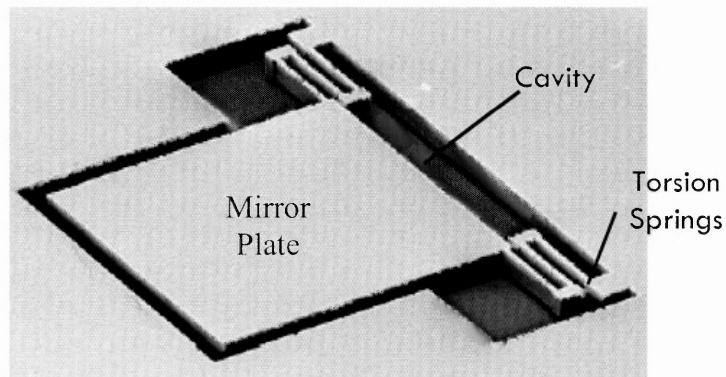


**Figure 3.1** The electrostatic microactuator (micro mirror).

The micro mirror was fabricated at the Microelectronics Research Center (MRC) at the New Jersey Institute of Technology (NJIT). It is fabricated in three stages. In the first stage, the cavity is formed by bulk anisotropic etching of the substrate. In the second stage, a thin silicon wafer is fusion bonded to the substrate to form a sealed cavity. Finally, the thin Si wafer is patterned in the region over the cavity by Deep Reactive Ion Etching to form the micromirror plate and torsion springs. A sketch of the whole fabrication process is available in the appendix.

### **3.2 Characterization**

The electrostatic microactuator is characterized to determine device dimensions, and for both static and dynamic behavior under applied bias. Static characteristics refer to the device deflection versus applied DC bias; and the dynamic characteristics refer to the resonant frequency, the mirror snap-down and snap-back voltages.

### **3.3 Microactuator Dimensions**

As the electrostatic microactuator is a mechanical device, the dimensions of the microstructure determine its dynamic characteristics. The following dimensions of the microstructure are measured.

1. Length of the mirror plate.
2. Width of the mirror plate.
3. Thickness of the mirror plate.
4. Depth of the cavity under the micromirror and spring.
5. Length of the springs.
6. Width of the springs.
7. Radius of curvature of the mirror plate.

The dimensions are measured using the WYKO profilometer. The WYKO profilometer works on the principle of optical interferometry to display the profiles of the test device, which is the electrostatic microactuator in this case. More information on optical interferometry is available in the appendix.

The images obtained from the optical profilometer will be as shown in Figure 3.2 below. These images are referred to as the 'profilometer images'.

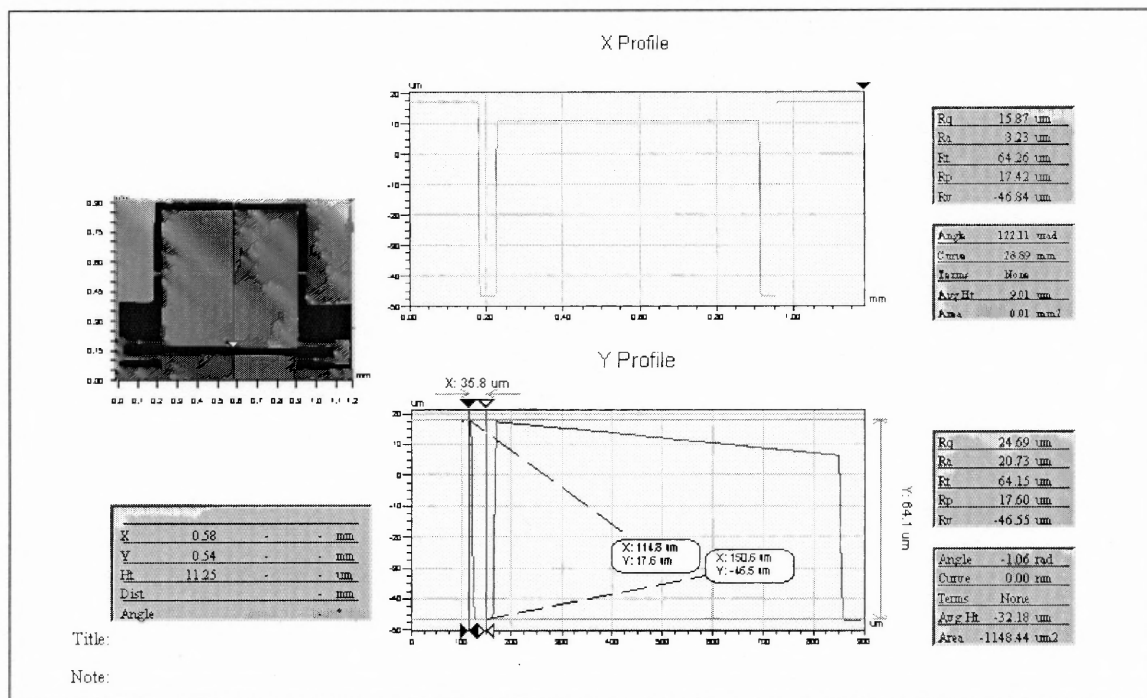
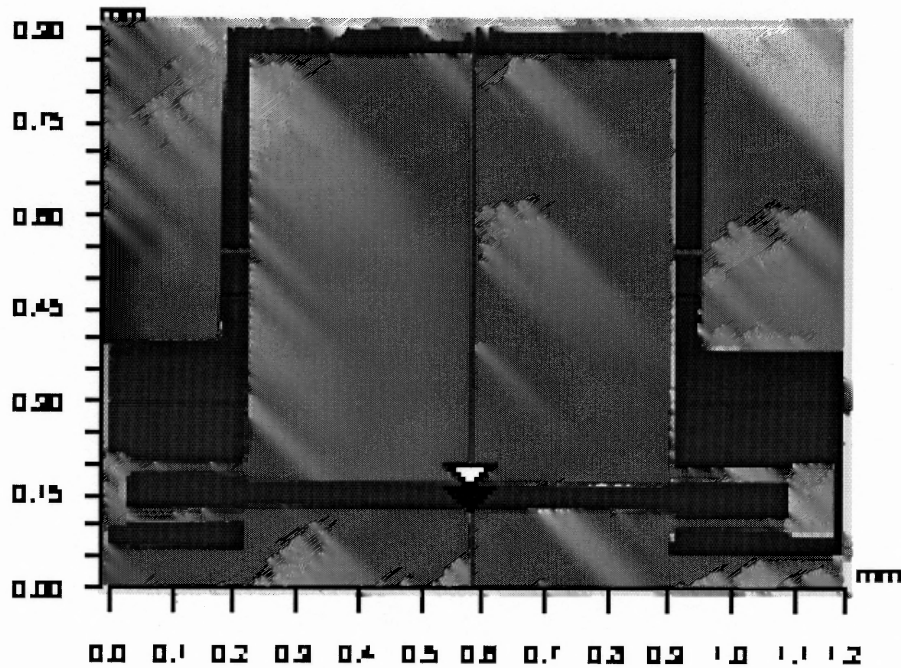


Figure 3.2 Profilometer image.

It consists of a top view of the structure and cross-sections. The top view is shown below in Figure 3.3.



**Figure 3.3** Top view of microactuator.

Since the top view is two-dimensional, the depth is indicated in shades of colors. The wavelength of the colors decreases with an increase in the depth. This means that the portions in Red (the mirror and springs) are at a higher elevation than the portions shown in Blue (the cavity).

The cross-sections are taken along both the X and Y axes and are known as the X and Y profiles respectively. The X profile will be as shown in Figure 3.4.

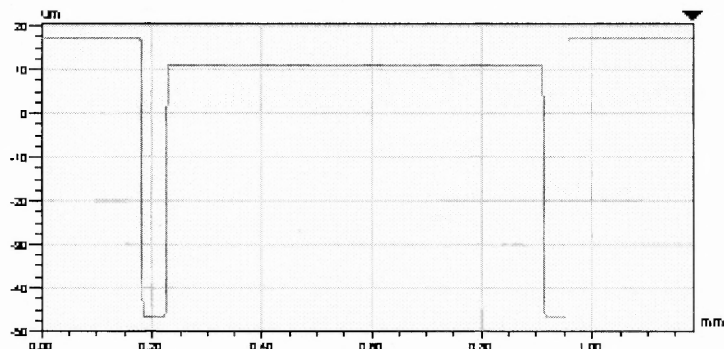


**Figure 3.4** X profile of microactuator.

The X-profile is the cross-section obtained along the Red (horizontal) line shown in the top view (Figure 3.3).

The Y profile will be as shown in Figure 3.5. The Y-profile is the cross-section obtained along the Blue (vertical) line shown in the top view (Figure 3.3).

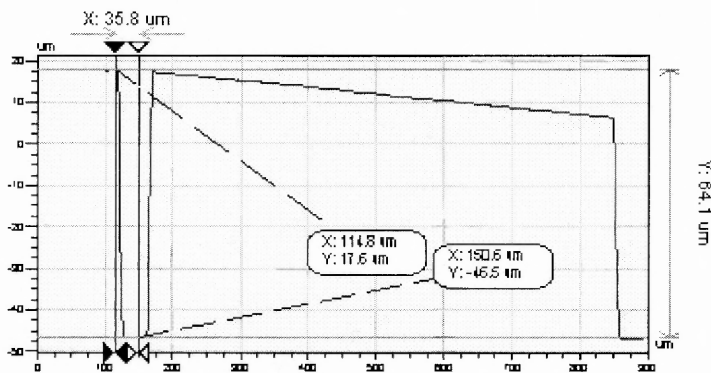


**Figure 3.5** Y profile of microactuator.

### 3.3.1 Dimensions of the Actuator Plate

The various portions of the electrostatic microactuator are illustrated in Figure 3.6.

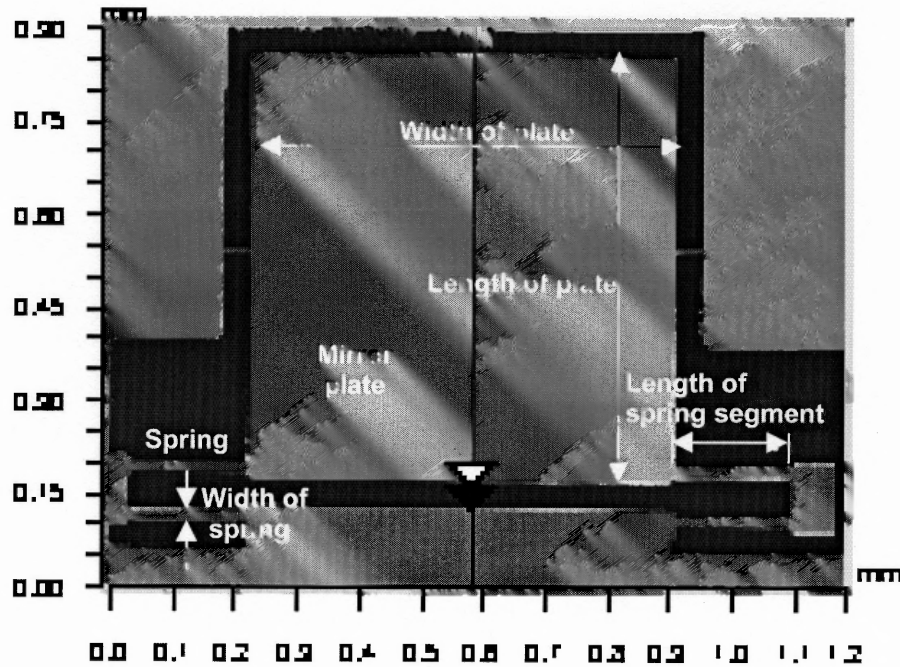


**Figure 3.6** Portions of the microactuator.

The dimensions illustrated in Figure 3.5, measured from the X and Y profiles are tabulated in Table 3.1 below.

**Table 3.1** Dimensions of the Microactuator

Portion	Profile	Dimension (in $\mu\text{m}$ )
Width of the plate	X	677.6
Length of the plate	Y	670



The thickness of the mirror plate cannot be measured from this profilometer image as a cavity is present under the mirror plate. Instead, the structure is physically forced to snapdown. The resulting profilometer image is shown below in Figure 3.7.

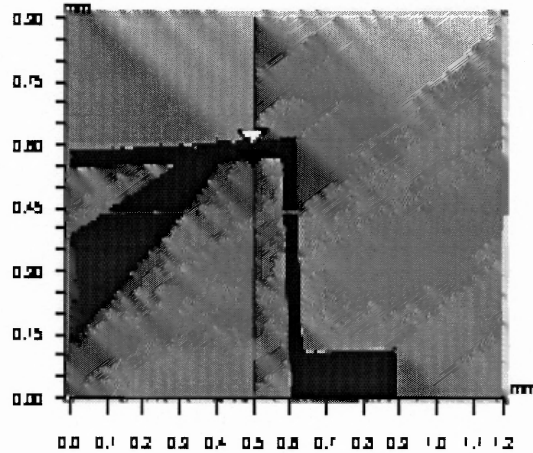


**Figure 3.7** Top view when the microactuator is in snapdown position.

The depth of the plate of the electrostatic microactuator is measured from the resulting Y profile, shown in Figure 3.8.

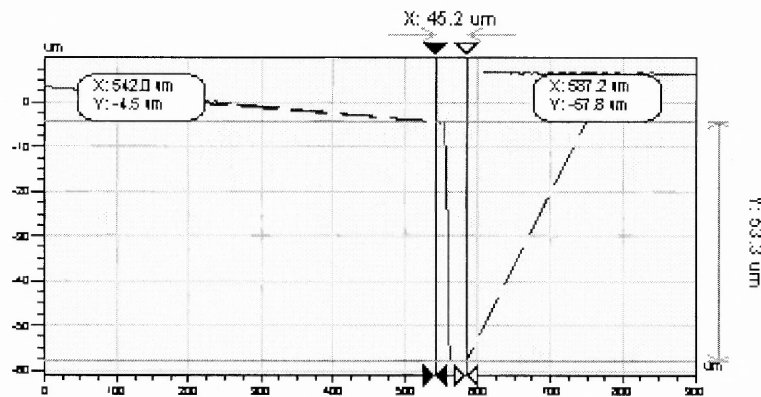


**Figure 3.8** Y profile of microactuator in snapdown position.

The depth of the electrostatic microactuator plate is  $53.3\mu\text{m}$ .

The depth of the cavity under the mirror plate cannot be measured directly. However, it can be determined as the difference in the height of the microactuator in its initial position (Figure 3.3) and when it is snapped down (Figure 3.7). The height of the mirror in its initial position is measured from the Y profile (Figure 3.5). This dimension is  $64.1\mu\text{m}$ . The height of the microactuator in its snapdown position is also measured from the Y profile obtained when the actuator is snapped down (Figure 3.8). This dimension is  $53.3\mu\text{m}$ . The depth of the cavity is the difference between these two dimensions i.e.,  $10.8\mu\text{m}$ .

### 3.3.2. Dimensions of the Actuator Spring

The dimensions of the actuator spring are measured by focussing on the spring alone. The resulting profilometer image is shown in Figure 3.9.

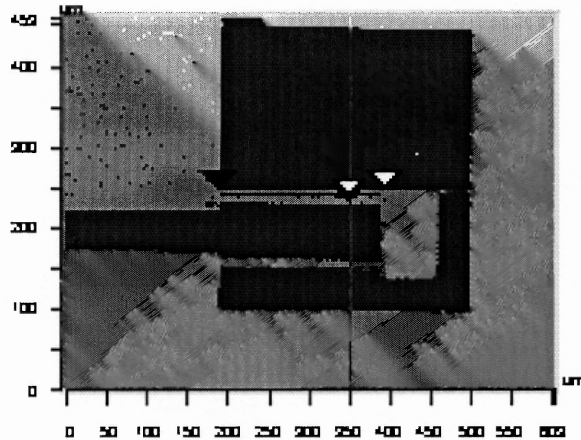


**Figure 3.9** Top view of actuator spring.

The spring is fabricated as a number of segments. The total length of the spring is calculated as the product of the number of segments and the length of each segment.

The length of each segment is is measured from the X profile of the actuator spring, shown in Figure 3.10. The length of each segment is  $207\mu\text{m}$ . The spring has two segments. Hence, the total length of the spring is  $414\mu\text{m}$ .

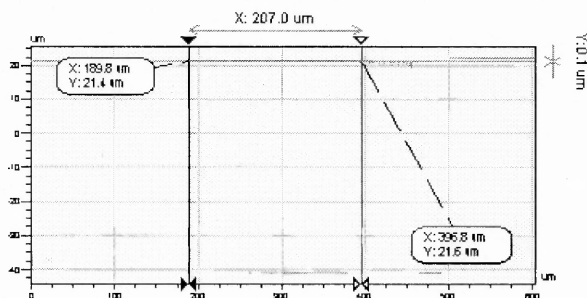


**Figure 3.10** X profile of actuator spring.

The width of the actuator spring is measured from the Y profile. The Y profile is shown in Figure 3.11. The width of the spring is  $8.6\mu\text{m}$ .

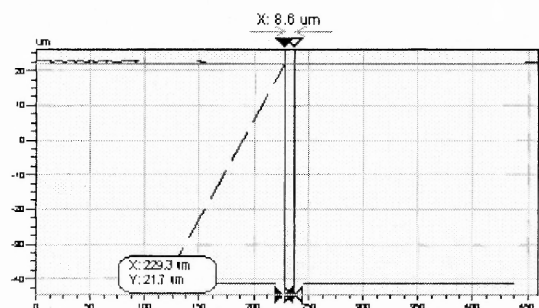


**Figure 3.11** Y profile of actuator spring.

The thickness of the spring is the same as the thickness of the mirror plate, which is  $53.3\mu\text{m}$ .

### 3.3.3 Resonant Frequency of the Microactuator

The resonant frequency of the microstructure is given by the following equation:

$$f = (0.44)^3 / (1 / (1 - 0.44 \times \beta) - 1 + \ln(1 - 0.44 \times \beta)) \quad (3.1)$$

where,  $\beta = 1$ . For the devices studied in this thesis, the resonant frequency exceeded 1 kHz, much greater than the inverse real-time image refresh rate.

## 3.4 Dynamic Characteristics of the Microactuator

### 3.4.1 Snapdown Voltage

The snapdown voltage of the microactuator is given by

$$V_{SD} = ((2 \times K_{\alpha} \times d^3) \times f / (\epsilon_0 \times a_3^3 \times b))^{0.5} \quad (3.2)$$

Where,

$$K_{\alpha} = (G \times w \times t^3 / 8 \times l) \times [(16 / 3) - (3.36 \times t / w) \times \{1 - (t^4 / 12 \times w^4)\}],$$

$$\beta = 1,$$

$$G = \text{Gauge factor for Si} = 0.73 \times 10^{11} \text{ Pa},$$

$$w = \text{thickness of the mirror plate} = 53.3 \mu\text{m},$$

$$t = \text{thickness of the spring} = 53.3 \mu\text{m},$$

$$l = \text{length of the spring} = 414 \mu\text{m},$$

$$d = \text{depth of the cavity} = 10.8 \mu\text{m},$$

$$\epsilon_0 = \text{Absolute permittivity} = 8.85 \text{ pF/m},$$

$$a_3 = \text{Length of the mirror plate} = 670 \mu\text{m},$$

$$b = \text{width of the mirror plate} = 677.6 \mu\text{m}.$$

For the dimensions measured, the calculated snapdown voltage,  $V_{SD} = 46.25 \text{ v}$ .

### 3.4.2 Experiment to Determine the Snapdown Voltage of the Microactuator

The voltage is applied between the actuator plate and the substrate. This arrangement is illustrated in Figure 3.12.

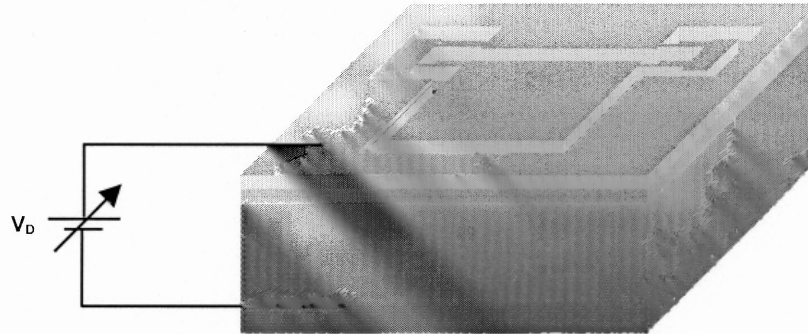


**Figure 3.12** Voltage is applied between the actuator plate and substrate.

The experimental setup to characterize the electrostatic microactuator for the deflection angle is shown in Figure 3.13.

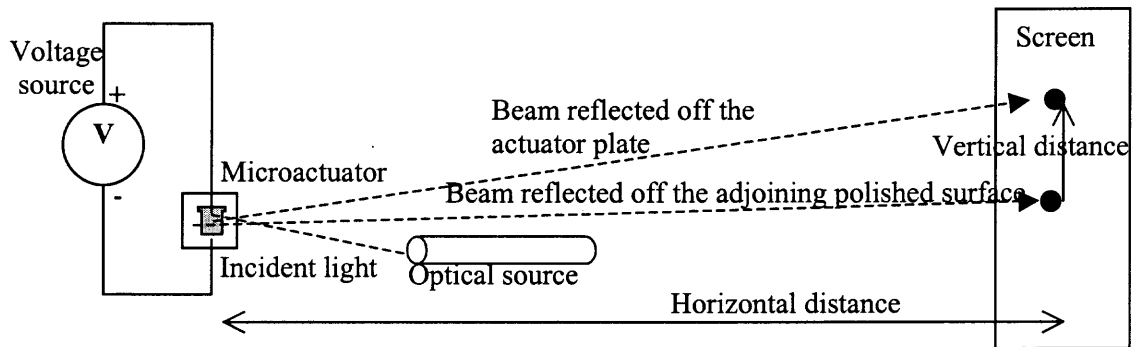


**Figure 3.13** Experimental setup to determine snapdown voltage of actuator.

The voltage is applied between the mirror plate and the substrate. The optical source throws light on the microstructure. This is indicated as the 'Incident light'. The reflected light falls on a screen. The distance between the actuator plate and the screen is measured. This distance is indicated as the 'Horizontal distance'. The light reflected off the surface of the micromirror forms a spot on the screen.

The Incident light falls on the ‘mirror plate’ as well as the ‘adjoining polished surface’, depicted in Figure 3.14.

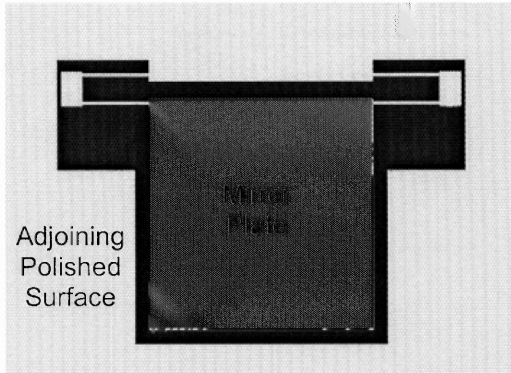


**Figure 3.14** Actuator plate and adjoining polished surface.

The light reflected off the mirror plate moves as the mirror deflects. As a result there are two spots. The distance between the two spots is the vertical displacement in Figure 3.13. The geometric analogy for the reflected beam is shown above in Figure 3.15.

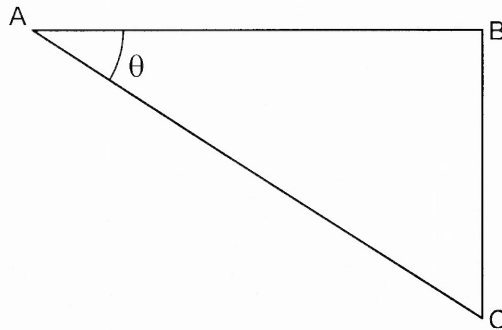


**Figure 3.15** Geometric analogy for the experimental setup.

The side AB represents the horizontal distance and the side BC represents the vertical displacement. The angle  $\theta$  is the angle of deflection.

The angle of deflection  $\theta$  can be calculated using the following relation.

$$\text{Tan } \theta = \text{BC} / \text{AB} \quad (3.3)$$

$$\therefore \theta = \text{Tan}^{-1}(\text{BC} / \text{AB}) \quad (3.4)$$

or

$$\theta = \text{Tan}^{-1}(\text{Vertical displacement} / \text{Horizontal distance}). \quad (3.5)$$

The maximum deflection angle is  $\sim 0.5$  degrees. From the experimental results, it is believed that the electrostatic microactuator is compatible for the application of LASER deflection.



## CHAPTER 4

### EYE TRACKING ALGORITHM AND GRAPHICAL USER INTERFACE

#### 4.1 Tracking Algorithms

The movement of the retina can be compensated using the following algorithms.

1. Exclusion area algorithm.
2. Eye tracking algorithm.
3. Hybrid algorithm.

In all the algorithms, the movement of the retina is tracked. A brief description of the algorithms is given below.

##### 4.1.1 Exclusion Area Algorithm

As the name signifies, the sensitive portions on the retina are selected as the “exclusion” areas before selecting the area to fire the LASER. As mentioned above, the movement of the eye is tracked. When the exclusion area (fovea) moves into the area where the LASER should be fired, the LASER will be disabled.

##### 4.1.2 Eye Tracking Algorithm

In this algorithm, the movement of the eye is tracked and followed. This means that if the eye moves, the LASER is also moved correspondingly, so that it always points to the area where it is aimed.

### 4.1.3 Hybrid Algorithm

In this algorithm, both the above-mentioned algorithms are incorporated. This means that once the operator selects an exclusion area, the LASER cannot be fired at the exclusion area.

In this thesis, the eye tracking algorithm has been implemented. The details on how the algorithm has been implemented, are discussed in the following chapters.

## 4.2 Aspects to Consider for Eye Tracking

### 4.2.1 Translation

This refers to the movement of the retina in the plane perpendicular to the axis of image capture. Figure 4.1 illustrates the translation motion of an image.

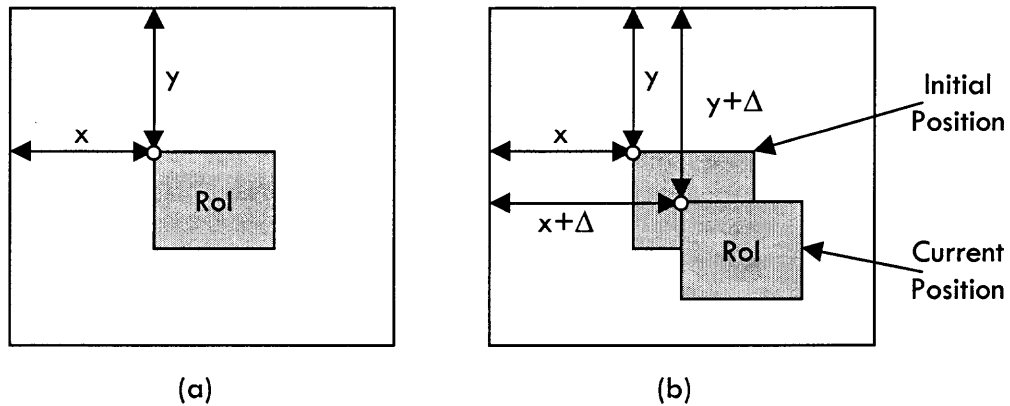


**Figure 4.1** The translation movement of an object. RoI is the Region of Interest.

The coordinates of the top-right corner pixel of the region of interest is  $(x, y)$ , as shown in Figure 4.1 (a). Due to translation, the region of interest moves from its initial position by  $\Delta x$  and  $\Delta y$  pixels in the  $x$  and  $y$  coordinates respectively. The new position for the RoI will be  $(x+\Delta x, y+\Delta y)$ , as shown in Figure 4.1 (b). This is the  $x$ - $y$  plane, perpendicular to the axis of image capture. The video camera captures the image of the region of interest (RoI) along the  $z$ -axis. Translation movement occurs because of the nystagmus.

### 4.2.2 Rotation

This refers to the torsion movement of the RoI along the axis of image capture. Figure 4.2 illustrates the rotation of the object.

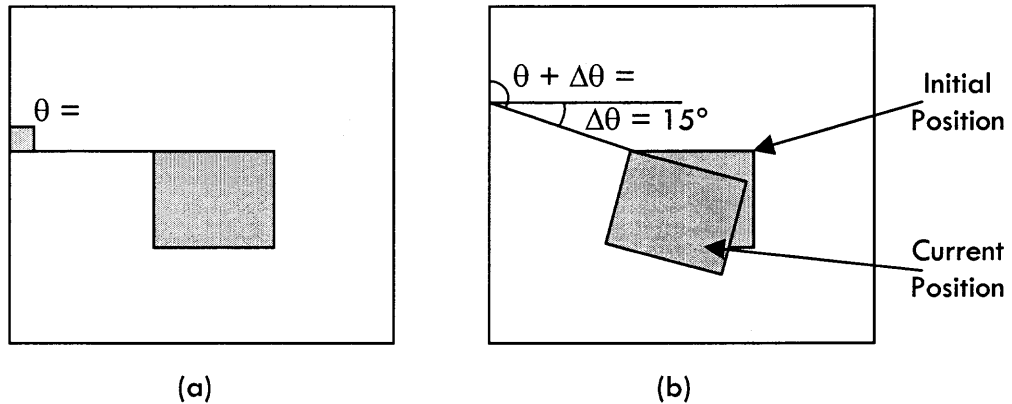


**Figure 4.2** The rotation of the object along the axis of image capture. The shaded region is the RoI.

Consider the RoI shown in Figure 4.2 (a). The RoI makes an angle of  $90^\circ$  with the x and y axes. Rotation would result in the RoI tilting away or towards the axes, as shown in Figure 4.2 (b). Along with the RoI, the rest of the image will also rotate. Rotation usually results when the patient is not properly positioned when performing the procedure.

### 4.2.3 Scaling

Scaling refers to the change in the size of the image from its initial size. This is illustrated in Figure 4.3.

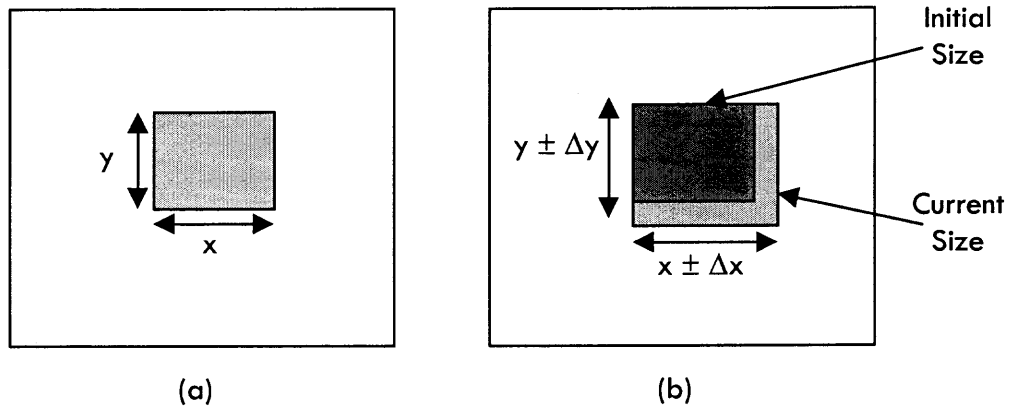


**Figure 4.3** Scaling of the image.

Consider Figure 4.3 (a). The initial size of the ROI is  $x \times y$  pixels. The image need not always be of the same size. It might increase or decrease to  $(x \pm \Delta x) \times (y \pm \Delta y)$  pixels. This is known as scaling. Scaling usually occurs because of the patient moving closer to or away from the video camera.

The scope of this thesis is to compensate of for the translation movement only. The rotation and scaling aspects have been discussed in the future work (Chapter 6).

As mentioned earlier (Chapter 1), the LASER eye surgery is a two-step process, where the fluorescein angiogram (FA) is obtained first, couple of weeks earlier to the actual procedure. The fluorescein angiogram and the retina, as observed in the microscope, will be different as shown in Figure 4.4.

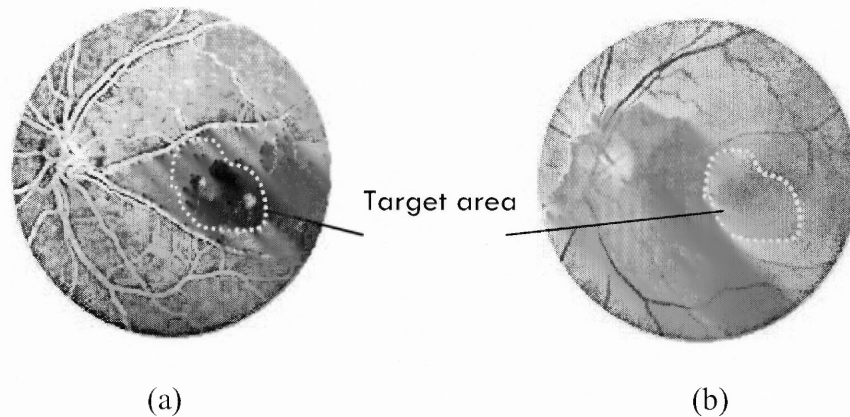


**Figure 4.4** Target area (Sub-Retinal-Neo-Vascularization) on the retina (a) fluorescein angiogram (b) microscopic image.

The operator identifies the SRNV (or target area) on the retina from the FA. The target area is highlighted with dotted lines in Figure 4.4. From Figure 4.4, it is clear that the target area is more clearly visible on the fluorescein angiogram (Figure 4.4 (a)), than on the microscopic image (Figure 4.4 (b)). As a result, the target area on the retina is identified from the FA. The corresponding target area on the microscopic image is identified by its relative distance from the features on the retina.

The features most conspicuously visible on the retina are the blood vessels; like the ones highlighted in Figure 4.5. The target area on the microscopic image is identified by observation.



**Figure 4.5** Reference areas on (a) fluorescein angiogram (b) microscopic image.

This means that an error on the part of the operator would result in striking the LASER on the wrong spot on the retina. The GUI is an attempt to prevent such eventualities.

The functions of the GUI are as follows:

1. Displays the fluorescein angiogram and the microscopic image of the retina.
2. Maps the fluorescein angiogram onto the microscopic image.
3. Allows the operator to select the target area.
4. Computes the amount by which the microscopic image is shifted with respect to the fluorescein angiogram.
5. Provides the correction factor for the X and Y directions.

### 4.3 Tracking the Eye

In all the three algorithms mentioned earlier, tracking of eye movement is essential. Tracking is performed by a process technically known as *registration*. Real-time registration involves considering a portion of a reference image (in this case, the fluorescein angiogram) and mapping it onto the corresponding features, grayscale values etc, on an acquired image (in this case, the real-time image). This is shown in Figure 4.6.

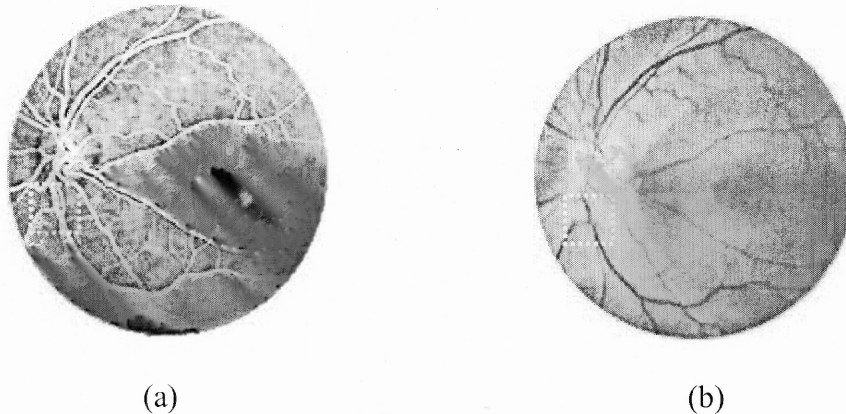


**Figure 4.6** Reference areas on (a) fluorescein angiogram (b) real-time image (RTI).

Consider the marked portions on the fluorescein angiogram and the real-time image. The features are the same. To map the real-time image onto the fluorescein angiogram, the highlighted regions in both the images have to be registered as the counterparts in the two images. These regions are known as the reference regions (or reference areas). Once the reference areas are registered, tracking of the real-time image can be accomplished by repeatedly mapping the newly acquired real-time image onto the fluorescein angiogram.



The difference in the pixel locations of the reference area on the fluorescein angiogram and the corresponding reference area on the real-time image is determined. This gives the amount, by which the LASER aiming beam should be offset, to aim at the desired target area.

#### 4.3.1 Registration

The images are stored as matrices of grayscale values. These grayscale values are used to perform the registration of the two images. Registration can be accomplished in two ways:

1. Sum of the squared differences.
2. Correlation.

Additional information on the algorithms is available in the appendix. The correlation algorithm is employed to perform the registration, as it is capable of performing feature mapping. The sum of the squared differences algorithm performs feature mapping only if both the images are the similar as shown in Figure 4.7.

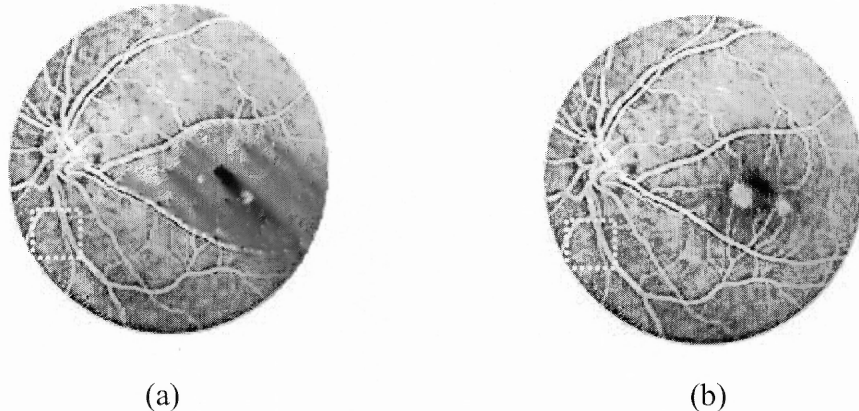


**Figure 4.7** Images should look identical for the sum of the squared differences algorithm to work with accuracy.

From Figure 4.6, it is clear that the fluorescein angiogram and the real-time image are not similar like the images in Figure 4.7.

### 4.3.2 Implementing the Registration

To perform registration, the both the images are stored in two matrices and registration is done with these values. Initially, the real-time image is a color image as shown in Figure 4.6 (b). The color image is made up of three components:

1. Red.
2. Green.
3. Blue.

The correlation algorithm will get too complicated if the fluorescein angiogram has to be registered onto the three matrices individually. However, the three matrices can be combined into a single matrix of grayscale values, using the equation<sup>[6]</sup> give below:

$$Y = 0.59 \times G + 0.30 \times R + 0.11 \times B \quad (4.1)$$

The resulting grayscale image would be as shown in Figure 4.8. In this image, the brighter the pixel, the higher the grayscale value. The grayscale values fall in the range (0, 255); 0 signifies Black and 255 signifies White.

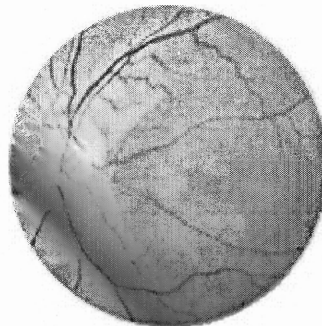


**Figure 4.8** Grayscale version of the real-time image.

When compared to the fluorescein angiogram, this image is like the inverted version of the fluorescein angiogram. However, this image can be further altered to match the fluorescein angiogram as close as possible. This alteration to be done is inverting the grayscale values. This means that a matrix  $Y^I$  will be used instead of  $Y$ . The relation between  $Y$  and  $Y^I$  is given by:

$$Y^I = 255 - Y \quad (4.2)$$

or

$$Y^I = 255 - (0.59 \times G + 0.30 \times R + 0.11 \times B) \quad (4.2)$$

The resulting image will be as shown in Figure 4.9. This image very closely resembles the fluorescein angiogram image.

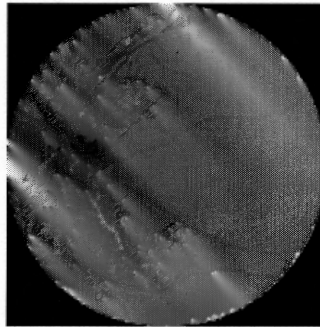


**Figure 4.9** Inverted grayscale version of the real-time image.

In this image, all the features are brighter, like in a fluorescein angiogram. This makes the correlation algorithm more accurate. These alterations are performed for each acquired real-time image.

#### 4.4 The Graphical User Interface

The Graphical User Interface (GUI) developed for the LASER eye surgery will be as shown in Figure 4.10.

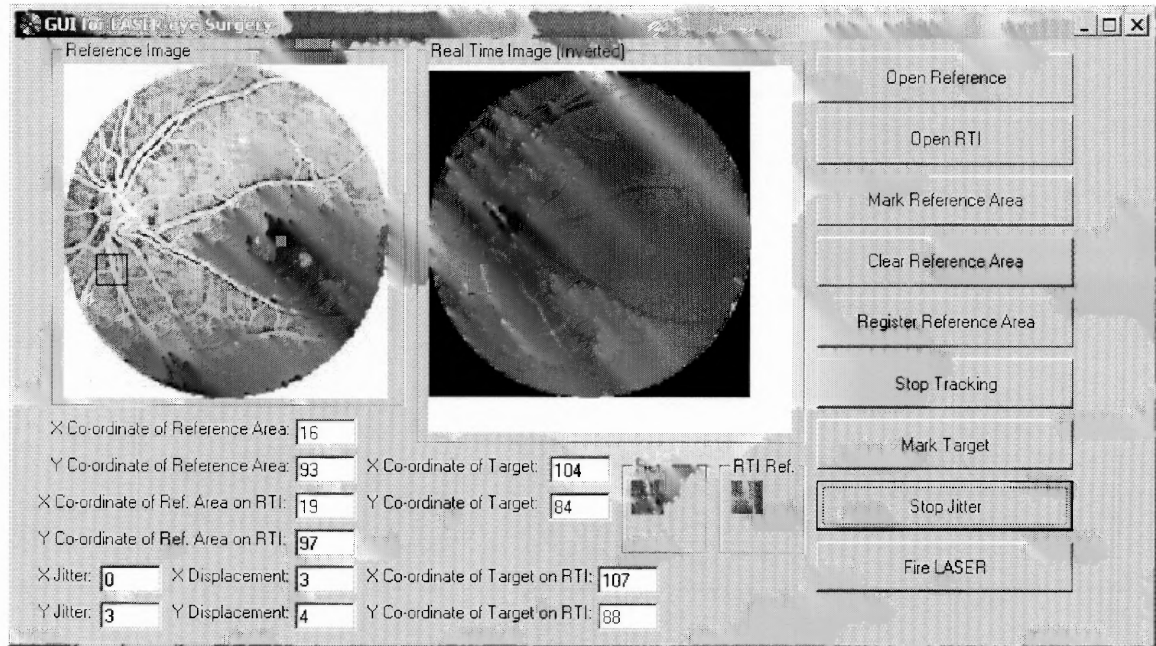


**Figure 4.10** The Graphical User Interface.

The “Reference Image” is the grayscale version of the Fluorescein Angiogram. The “Real Time Image” is the grayscale version of the RTI. The procedure to use the GUI is as follows.

1. The grayscale values of the FA and the RTI are stored in files. The images should be drawn from the files. The “Open Reference” and “Open RTI” buttons should be clicked to open the FA and the RTI respectively. The RTI should now be registered on the FA.
2. The reference area should be marked on the FA by clicking “Mark Reference Area” and placing the selection box on the desired area on the FA.

3. The area outlining the corresponding reference on the RTI should be marked by clicking the “Register Reference Area” and placing the outlining box on the RTI. On doing so, the GUI registers the RTI onto the FA and displays the reference areas of the FA and RTI in the “Ref.” And “RTI Ref.” boxes, respectively.

Tracking and jitter can be toggled ON or OFF by clicking the “Start/Stop tracking” and “Apply/Stop Jitter” buttons respectively. Two independent subroutines apply jitter and track the image. The (X, Y) coordinates of the reference areas on the FA and RTI are displayed. The GUI is a simulation to prove that the correlation and the sum of squared difference methods perform proper registration. The following observations can be made from this simulation:

1. The accuracy of the GUI depends on the features selected for the reference area.
2. The method of sum of squared differences works well if both the images look identical. It does not work if the RTI looks different from the FA.
3. The correlation algorithm works well for feature registration. This means that correlation would work even if the RTI does not have the same grayscale values, but have the same features.

## **CHAPTER 5**

### **CONCLUSION**

This thesis has developed a system for laser eye surgery that is a significant improvement over existing technology. The new system uses image matching and MEMS micromirrors to introduce feedback control, automation and record keeping to the laser surgery process, eliminating the unwanted effects of eye movement during surgery and introducing a wide range of other benefits. It is expected that this improvement can be implemented as an addition to existing systems as well as a foundation for new tools, perhaps even remote, internet enabled ones. While macular degeneration has been a target application discussed in this work, extension is possible to the treatment of other diseases such as diabetic edema.

The basic components of the new system have been described and demonstrated, including image matching between reference and real-time images through well-known algorithms, application of matching information to generate control voltages to lock positioning and firing LASER onto selected locations on the eye using electrostatically controlled micromirrors, and characterization of the micromirrors for this application. A particular focus of this thesis has been the development of a prototype graphical user interface that integrates image capture, image matching, mirror control, and user interaction into a single unit.

## **CHAPTER 6**

### **FUTURE SCOPE**

The scope of this thesis has been limited to proving a concept. Future work should address additional features that should be considered when implementing an actual system for surgical use. Several of these features are described below.

#### **6.1 Aspects of Retinal Movement**

In this thesis, the only aspect of retinal movement considered is translation using matching to a single region of the eye. Rotation, scaling, and skewing have been ignored (Chapter 4). When incorporating these aspects, more complex algorithms, and additional match regions will be required for the tracking algorithm. Dedicated algorithms or packages like MATLAB<sup>[7]</sup> may be useful for the more complex matching purposes.

#### **6.2 Incorporating the CALS in the Existing Surgical Equipment**

Methods of incorporating the setup in existing LASER surgical equipment have to be investigated. This includes development of the design and positioning of parts such as the MEMS deflection mechanism and package, distance between the MEMS mirrors responsible for the vertical and horizontal deflection, distance of MEMS components from the eye, protocols for operation such as mirror calibration procedures if needed, etc. Additional mirror characterization work will be required in order to assure repeatable and reliable performance.

## **6.3 Additional Features in the Graphical User Interface**

### **6.3.1 History of Surgical Procedure**

When using Argon Green or Krypton Red lasers (as assumed in this thesis), the LASER is visible and the treated regions show up immediately. In some cases, a diode LASER might have to be used. The diode LASER is not visible. This problem can be overcome by including a feature that would store information on the regions where the LASER has been fired. Whenever required, the operator would bring up an image that shows the regions already treated.

### **6.3.2 Computer Controlled LASER**

An interface to control the LASER can be incorporated. This will allow the operator to program the LASER settings or to choose between several different lasers.

### **6.3.3 More User-Friendly Graphical User Interface**

The above mentioned features will be more useful if the Graphical User Interface can be programmed for specific patient conditions, surgical procedures and LASER specifications. These and other improvements will be a natural outgrowth of further development of this thesis work.



## 6.4 Remote Operation

An intriguing possible outcome of this work may be the ability to view or conduct surgery via the Internet. While a patient handler would be required at the treatment clinic, the automation enabled by this system allows the surgery to be viewed or performed remotely.

## **APPENDIX A**

### **MACULAR DEGENERATION**

The retina is a tissue in the back of the eye. It is an extremely complex structure that contains millions of cells. The macula, an area of approximately 1/4 inch in diameter, is the central part of the retina and is responsible for central or straight ahead vision. The term macular degeneration, therefore, implies a disease in which a degenerative or aging process affects this particular area.

The macula contains a very small central area called the fovea. It is this part of the macula which is responsible for very sharp vision. Thus, if only a part of the macula is diseased but the fovea is intact, vision can still be good.

When rays of light enter the eye, they first pass through transparent structures – the cornea, the lens and the vitreous. Light rays are then focused on that part of the macula called the fovea. The fovea is different from the rest of the retina, since it contains a very high concentration of cells called cones. Because of this, the fovea is the only area of the retina capable of 20/20 vision. Since the cones must have bright light to function normally, the fovea works best in daylight illumination. The rest of the retina, including the macula area outside the fovea, has another type of receptor called the rod. The rod functions better in dim illumination and is not capable of sharp central vision.

Behind the retina is another tissue called the choroid, which is a very vascular tissue. Between the retina and the choroid is a space called the subretinal space. Abnormal blood vessels from the choroid grow into the subretinal space in age-related macular degeneration. This growth of blood vessels leads to bleeding and scarring which is responsible for the vision loss in age-related macular degeneration.

Age-related macular degeneration (AMD) is the leading cause of severe, irreversible vision loss. It is predominantly due to the age-related process, although certain patients have a genetic pre-disposition. The disease is most commonly seen in patients who are 50 years of age or older. It is seen in increasingly greater frequency as the population gets older. Other factors that have been suggested, besides aging and genetics in causing this disease, include chronic sunlight exposure and nutrition. However, overwhelmingly, the most important factors in the development of macular degeneration are the aging process and hereditary.

The most common symptom of abnormal blood vessel growth from age-related macular degeneration is distortion, waviness, or a smudge like area in the central vision. Patients may notice these changes when looking at objects with straight edges, like the sides of a building, or the tile on their floor. They may be given an Amsler grid <sup>[9]</sup> by their doctor to check this sensitive central area of the retina.

## APPENDIX B

### FABRICATION OF THE MEMS MIRROR

The MEMS electrostatic microactuator is fabricated using two independent wafers. The sketch of the fabrication process for the MEMS electrostatic microactuator is given below.

A cavity is etched on one of the wafers by photolithography. This results in a pit as shown in Figure B.1. This pit forms the cavity under the actuator plate.

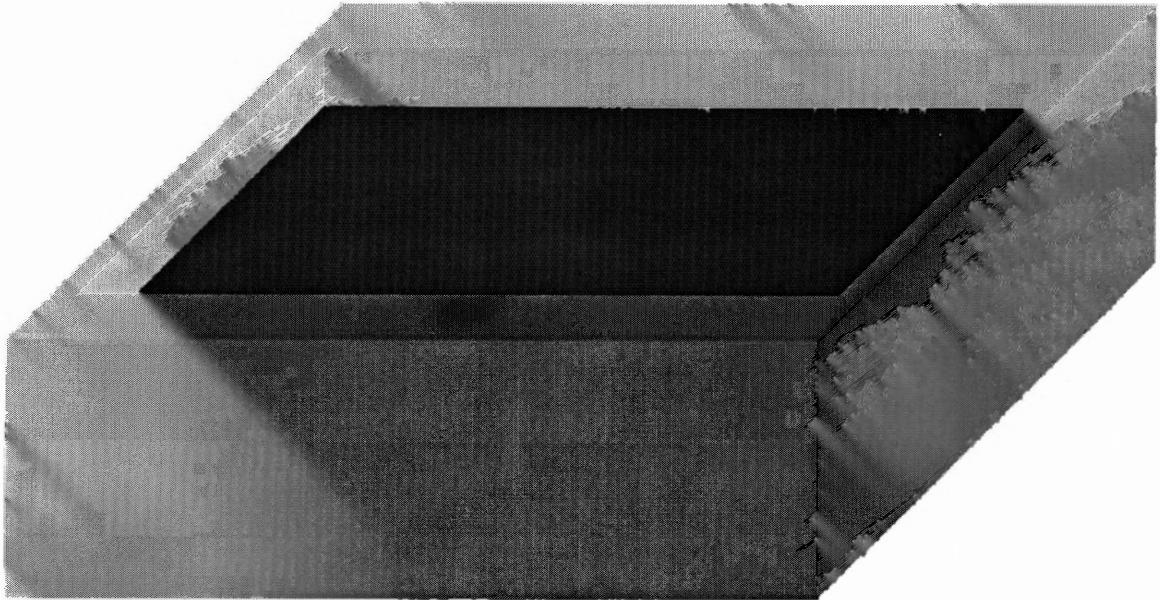


**Figure B.1** Etched pit on the Silicon wafer. This forms the cavity under the actuator plate.

Silicon Dioxide ( $\text{SiO}_2$ ) is grown over the structure. This  $\text{SiO}_2$  forms the insulating material between the actuator plate and the substrate. Figure B.2 illustrates this well.

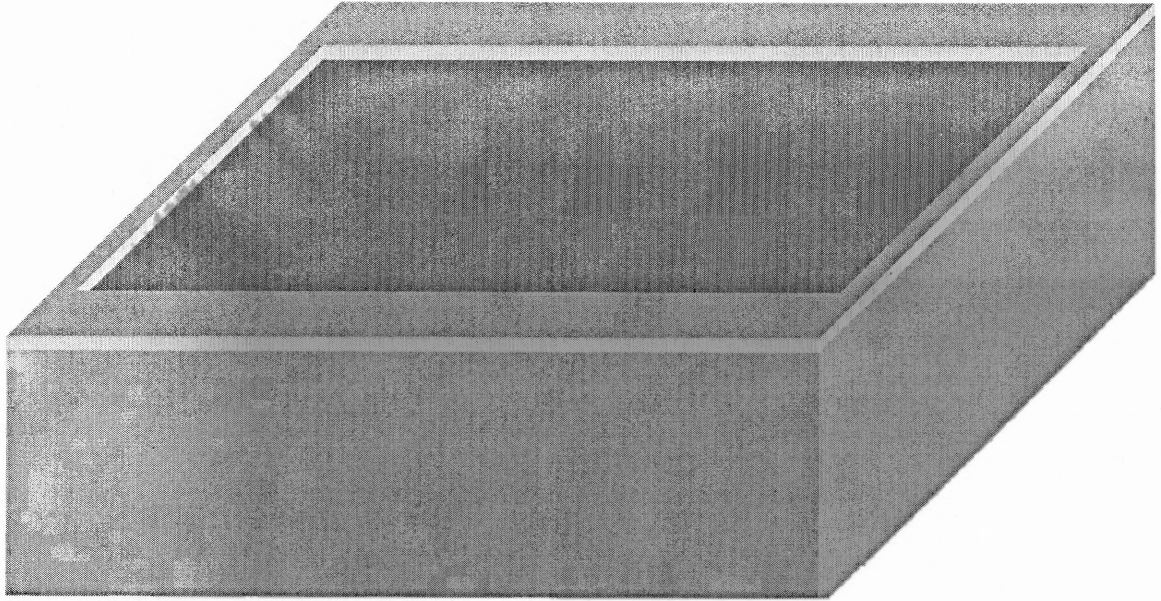


**Figure B.2** Growth of  $\text{SiO}_2$  on the wafer.

$\text{SiO}_2$  is also grown on a thin single crystal Silicon wafer. This thin Silicon wafer forms the actuator plate. After growth of  $\text{SiO}_2$ , the actuator plate looks as shown in Figure B.3.

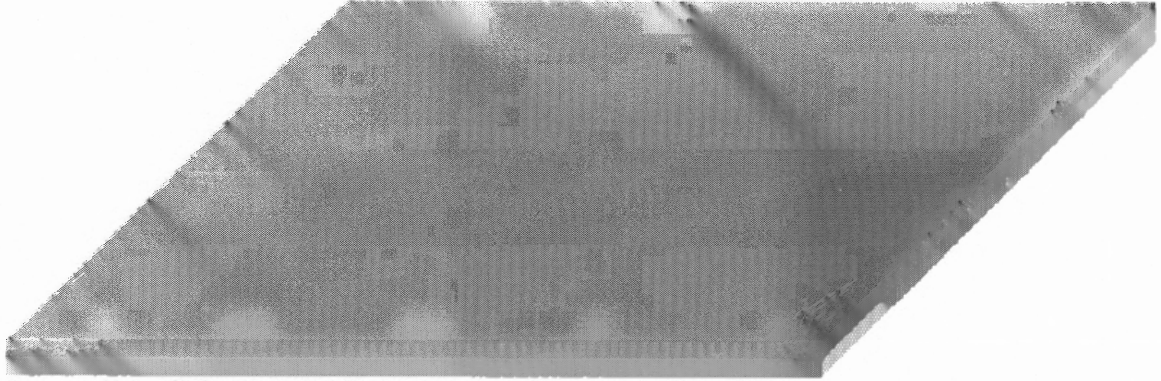


**Figure B.3**  $\text{SiO}_2$  is grown on a thin Silicon wafer. This makes the wafer bonding easier.

This thin Silicon wafer is fusion bonded to the first Si wafer, on which a cavity was etched, resulting in a sealed cavity as shown in Figure B.4.

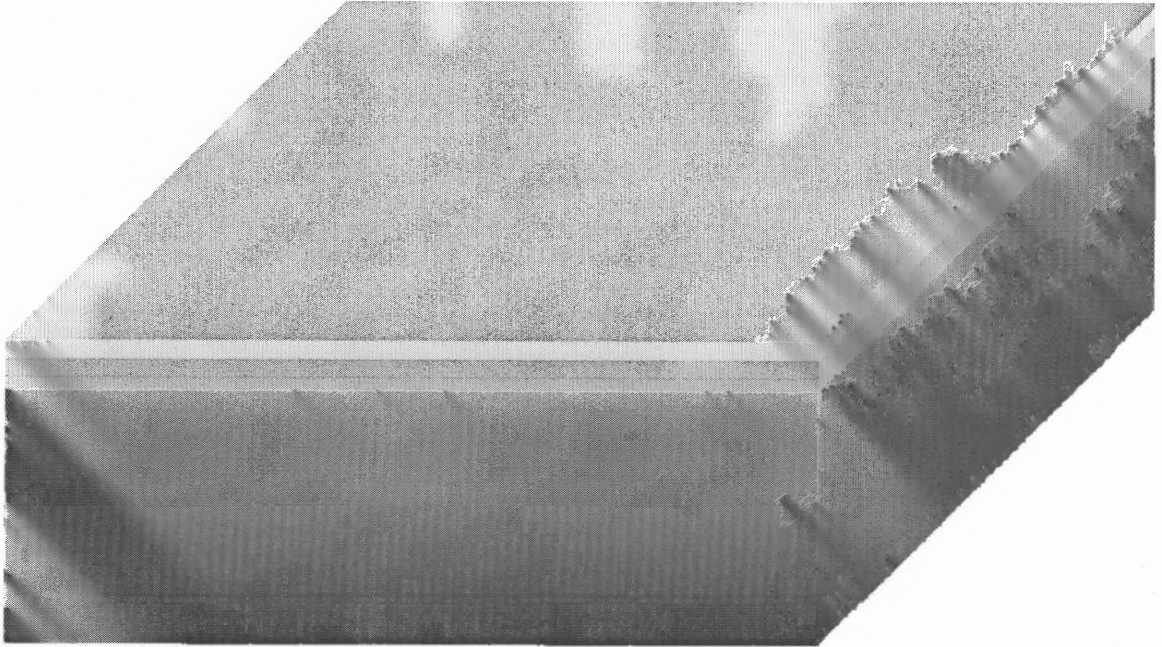


**Figure B.4** The thin Silicon wafer is fusion bonded to the first wafer.

The shape of the actuator plate is patterned on the thin Silicon wafer. The resulting pattern will be as shown in Figure B.5

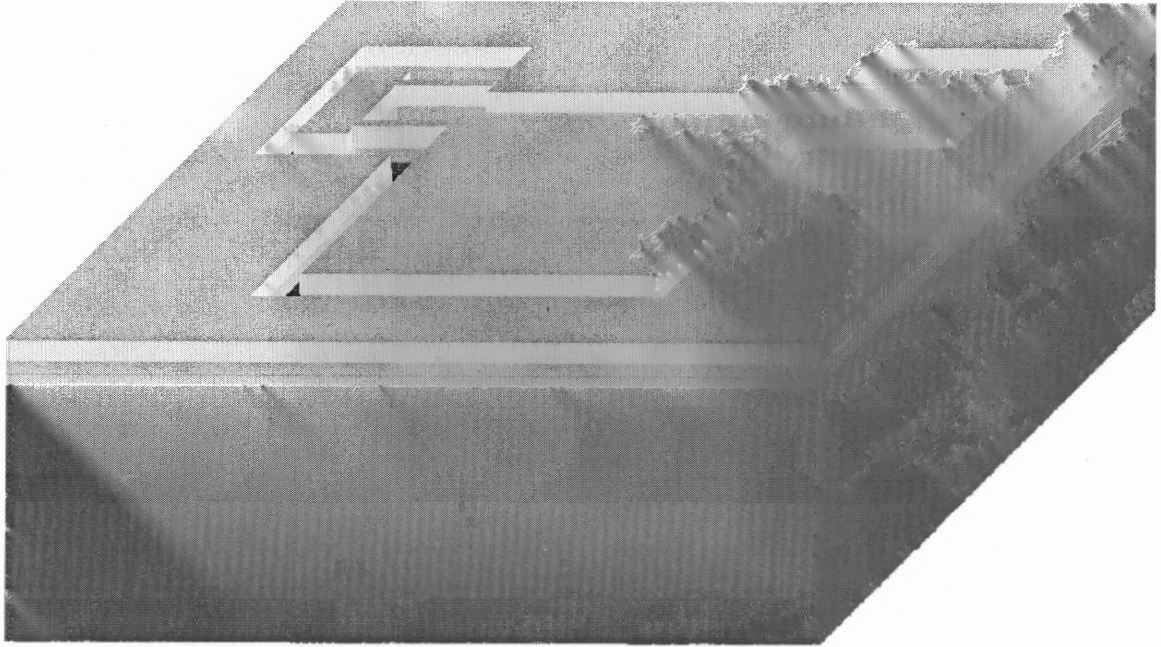


**Figure B.5** Actuator plate patterned on the bonded thin Silicon.



Finally, Chromium and Gold are deposited on the actuator to provide a polished surface and a good top electrical contact. The resulting structure will be as shown in Figure B.6.

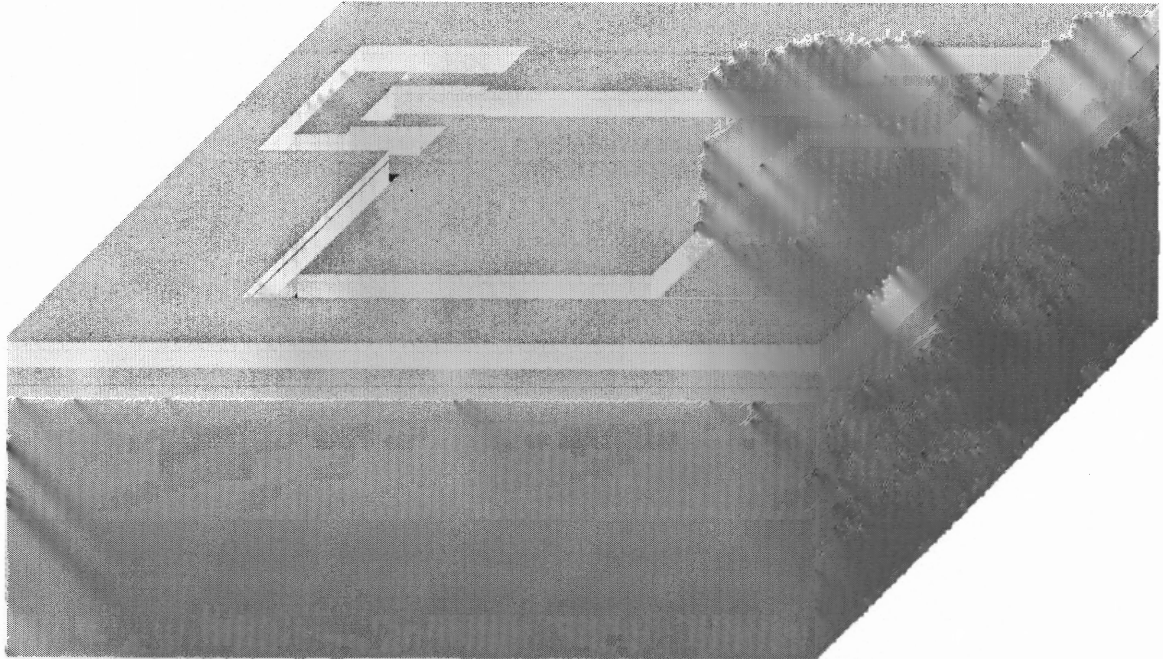


**Figure B.6** Gold and Chromium deposition on the actuator structure, to provide a polished surface and good electrical contact.

**APPENDIX C**  
**REGISTRATION ALGORITHMS**

Two algorithms have been tried to perform registration.

1. Sum of squared differences

$$D(m, n) = \sum_{i=0}^{i=9} \sum_{j=0}^{j=9} (FA(i, j) - RTI(m+i, n+j))^2, m = x \text{ to } x^l, n = y \text{ to } y^l \quad (A.1)$$

2. Correlation

$$C(m, n) = \sum_{i=0}^{i=9} \sum_{j=0}^{j=9} \frac{FA(m+i, n+j) \times RTI(m+i, n+j)}{\{FA(m+i, n+j)^2 \times RTI(m+i, n+j)^2\}^{0.5}}, m = x \text{ to } x^l, n = y \text{ to } y^l \quad (A.2)$$

Where,

FA is the matrix of grayscale values of the fluorescein angiogram

RTI is the matrix of grayscale values of the real-time image

x is the x coordinate of the pixel where the scanning begins in FA

y is the y coordinate of the pixel where the scanning begins in FA

$x^l$  is the x coordinate of the pixel where the scanning ends in FA

$y^l$  is the y coordinate of the pixel where the scanning ends in FA

The reference area on the fluorescein angiogram was a  $10 \times 10$  matrix. As a result, in the above equations, i and j vary in the range (0, 9). The observation made is that the sum of squared differences algorithm works best if the two images are identical. However, this is not the case with the correlation algorithm. In this thesis, the correlation algorithm has been used to perform registration.

## REFERENCES

1. <http://www.vrmny.com/AMD.htm>, October 2002.
2. <http://www.lasertech.com/pulselaser.html>, October 2002.
3. <http://www.vecpa.com/index.cfm/procedures/photodynamictherapy>, September 2002.
4. Gregory T. A. Kovacs. "Micromachined transducers sourcebook", McGraw Hill publications, 1994.
5. R. A. Brown, V. A. Aksyuk and K. R. Farmer. "Micromachined, electrostatically actuated optical attenuators / switches fabricated by fusion bonding of single-crystal, ultra-thin Silicon wafers", Proceedings of the 5th International Symposium on Semiconductor Wafer Bonding: Science, Technology and Applications, Honolulu, Hawaii, October 17-22, ECS Proceedings Vol. 99-35, 1999, p. 407.
6. <http://www.scantips.com/lumin.html>, February 2003.
7. <http://www.maculardegeneration.org/enroll.html>, November 2002.
8. <http://www.vrmny.com/amsler.htm>, October 2002.